

**Interference between bulk and boundary scattering in high quality films**

S. Chatterjee and A. E. Meyerovich

*Department of Physics, University of Rhode Island, Kingston, Rhode Island 02881, USA*

(Received 29 March 2010; revised manuscript received 12 May 2010; published 7 June 2010)

Quasiclassical interference between bulk and boundary scattering channels in thin metal films with rough surfaces is discussed. The effective transport time, which is calculated beyond Mathiessen's approximation, exhibits a nonanalytical dependence on the bulk relaxation time. Interference effects strongly affect the temperature (phonon scattering in the bulk) or concentration (impurity-scattering) dependencies of the conductivity. The results for large bulk free paths  $\mathcal{L}_b$  and large correlation radii (lateral sizes)  $R$  of surface inhomogeneities are described by simple analytical equations. At  $R^2 \sim a\mathcal{L}_b$  we predict a crossover between two asymptotic regimes for interference contributions that are characterized by distinct temperature/concentration dependencies. Experimental implications of our results are discussed.

DOI: [10.1103/PhysRevB.81.245409](https://doi.org/10.1103/PhysRevB.81.245409)

PACS number(s): 73.23.Ad, 73.50.Bk

**I. INTRODUCTION**

Rapid progress in material science, vacuum and low-temperature technologies, system miniaturization, etc., leads to proliferation of ultraclean miniature systems such as ultrathin metal films in which the boundary scattering becomes equally or even more important than the bulk scattering. The wall scattering involves an entangled combination of processes of different physical nature such as changes in energy spectra near the walls, stick-slip motion and partial accommodation, scattering by surface roughness and impurities, surface states, etc. What is more, various bulk and surface-scattering processes are not necessarily independent but can interfere with each other. For example, when scattering is weak, as it is often the case for electron-phonon scattering or scattering by slight surface roughness, the establishing of mean free path requires several scattering events. As a result, the transport properties become sensitive to the order of scattering events involving various channels. In clean metal films at not very low temperatures the main bulk channels are the electron-phonon scattering, scattering by grain boundaries and by residual impurities. Below we assume that the density of grain boundaries is relatively small and concentrate either on electron-phonon processes or on scattering by impurities. For surface scattering, we assume that the main scattering effects result from scattering by surface roughness. We will look at the interference between bulk and roughness scattering in electron conductivity beyond the Mathiessen's rule. The main goal is to search for an unusual dependence of conductivity on temperature or impurity concentration which could be a signature of such interference. An auxiliary goal is to find a way of extracting parameters of surface roughness from experimental data on conductivity.

A usual approach to transport in films is to account for bulk-scattering processes via a collision operator in a transport equation and to relegate all boundary scattering to some phenomenological boundary condition (for one of the best known examples of earlier work in this direction see Ref. 1). One of the tasks then is to express the phenomenological parameters in this boundary condition (such as, for example, the specular coefficient  $p$  or the Namba<sup>2</sup> ratio of the amplitude of roughness and the mean free path,  $\ell/\mathcal{L}_b$ ) via

physical characteristics of surface. There are two issues with such an approach. First, the choice of the *form* of the boundary condition by itself imposes limitations, which are not always clear, on what kind of surface physics can or cannot be properly incorporated by this condition. The second issue is mathematical. Since bulk and surface-scattering processes are accounted for within different mathematical frameworks—the former by the bulk-collision operator and the latter as the boundary condition—one should always expect certain entanglement between surface and bulk scattering in the transport results obtained this way. It is not always clear to what extent the emerging non-Mathiessen's terms reflect real physical interference between different scattering processes and not just some mathematical artifacts.

More recently, there appeared an alternative approach to boundary scattering, or, more precisely, to scattering by surface roughness which in some experiments accounts for almost half of the overall resistivity of nanosystems.<sup>3</sup> The approach is based on a mapping transformation technique, which in application to transport problems was originally developed in Refs. 4–6. The approach involves mapping of a system with random rough boundaries onto an equivalent physical system with ideal boundaries but distorted bulk Hamiltonian. This allows one to incorporate the scattering by surface roughness into the same type of collision operator as for bulk-scattering processes. Though this is not the only approach to scattering by surface roughness (see a short review in the second Ref. 7), it became clear from the very beginning that the mapping transformation is valuable for simultaneous description of bulk and surface-scattering channels including the interference non-Mathiessen's terms (see the second Ref. 4). The mapping transformation approach allows one not only to develop a mathematically rigorous derivation for the bulk quantum transport equation and the collision operator, which reflects the boundary roughness in the initial problem, but also to understand the limitations and accuracy of alternative approaches to the problem.<sup>7</sup>

With the help of mapping transformation, all bulk and surface-scattering channels can be treated in the same way within the single quantum transport formalism. Since now all scattering channels are treated in the same way, the results should reveal the real physical interference between bulk and surface scattering in transport. Based on this approach, in

Ref. 8 we developed a rigorous diagrammatic derivation of the quantum transport equation for particles in quantized films with bulk and boundary scattering.

A somewhat similar, though technically different quantum approach based on the surface-scattering model of Ref. 9 has been outlined in Refs. 10 and 11 in the white-noise approximation for a rough surface. This approach corresponds to adding the surface scattering as a perturbation of the type<sup>9</sup> to the single-particle Green's function which already includes the bulk scattering. In diagrammatic language, this corresponds to adding a surface interaction line on top of the propagator with bulk interaction (bold line). Such an approach excludes from the outset all the diagrams with the intersecting bulk and surface interaction lines that were included in Ref. 8.

Below we apply our quantum transport approach<sup>8</sup> to the non-Mathiesen's terms that arise from quasiclassical interference between bulk and surface scattering. We will also try to compare our results with (scarce) experimental data on non-Mathiesen's contributions. The next step should be to find out to what extent it is even possible to incorporate the scattering by surface roughness, including the surface-bulk interference effects, into a boundary condition. Below we will just touch this issue by comparing our results with the Fuchs-Sondheimer equations<sup>1</sup> and getting the expression for the specularly coefficient via the roughness profile.

## II. MAIN EQUATIONS

An important feature of ultrathin films is the quantization of motion across the film,  $p_{zj} = \pi j \hbar / L$ , where  $L$  is the thickness of the film. This quantization, which is responsible for quantum size effect (QSE) in transport, leads to a split of the three-dimensional spectrum  $\epsilon(\mathbf{p}) = p^2 / 2m$  into a set of two-dimensional minibands  $\epsilon_j(\mathbf{q})$ , where  $\mathbf{q}$  is the component of momentum along the film. In the simplest case of parabolic spectrum with effective mass  $m$ ,  $\epsilon(\mathbf{p}) = p^2 / 2m$ , the minibands are also parabolic,  $\epsilon_j(\mathbf{q}) = (1/2m)[(\pi j \hbar / L)^2 + q^2]$ . Under certain realistic conditions, which have been analyzed in Ref. 8 in detail, the diagrammatic equations for the full single-particle Green's functions, which include both bulk and surface scattering, contain the following imaginary part in the energy denominator which we call the effective relaxation time  $\tau_j^{(eff)}(\mathbf{q})$  for particles from each miniband  $\epsilon_j(\mathbf{q})$  [cf. Ref. 10]

$$\frac{1}{\tau_j^{(eff)}(\mathbf{q})} = \frac{1}{\tau_j^{(b)}(\mathbf{q})} + \sum_{j'=1}^S \int \frac{W_{jj'}(\mathbf{q}, \mathbf{q}') / \tau_{j'}^{(b)}(\mathbf{q}')}{[\epsilon_{j'}(\mathbf{q}') - T_F]^2 / \hbar^2 + [1/2 \tau_{j'}^{(b)}(\mathbf{q}')]^2} \times \frac{d\mathbf{q}'}{(2\pi\hbar)^2}. \quad (1)$$

Here  $S$  is the total number of occupied or energetically accessible minibands  $\epsilon_j(\mathbf{q})$  and  $\tau_j^{(b)}(\mathbf{q})$  is the bulk relaxation time in each miniband  $\epsilon_j$  which should be treated not as a phenomenological parameter, but as an unambiguously defined imaginary part in the denominator of the single-particle Green's function for unrestricted bulk. In our context, the bulk parameters  $\tau_j^{(b)}(\mathbf{q})$  are determined by electron-phonon

or impurity scattering in the bulk and are considered known. The wall-induced transition probabilities  $W_{jj'}(\mathbf{q}, \mathbf{q}')$  between states  $\epsilon_j(\mathbf{q})$  and  $\epsilon_{j'}(\mathbf{q}')$  are determined by the correlation functions of surface inhomogeneities on both walls,  $\zeta_{11}$  and  $\zeta_{22}$ , and by the interwall correlation of surface inhomogeneities  $\zeta_{12}$ , Ref. 7. When the metal film can be treated as a two-dimensional square well, the equations for these transition probabilities are quite simple

$$W_{jj'}(\mathbf{q}, \mathbf{q}') = \frac{\pi^4 \hbar^2}{m^2 L^6} [\zeta_{11}(\mathbf{q} - \mathbf{q}') + \zeta_{22}(\mathbf{q} - \mathbf{q}') + 2(-1)^{j+j'} \zeta_{12}(\mathbf{q} - \mathbf{q}')] j^2 j'^2. \quad (2)$$

Though most of the calculations can be performed for any type of surface correlator, here we assume that the correlations of inhomogeneities on both walls are identical  $\zeta_{11} = \zeta_{22}$  and Gaussian,

$$\zeta(\mathbf{s}) = \ell^2 \exp(-s^2 / 2R^2), \quad \zeta(\mathbf{q}) = 2\pi \ell^2 R^2 \exp(-q^2 R^2 / 2\hbar^2), \quad (3)$$

where  $\ell$  and  $R$  play the role of the amplitude (height) and correlation radius (lateral size) of surface inhomogeneities and that there are no interwall correlations,  $\zeta_{12} = 0$ . (The Gaussian peak in the  $\delta$ -function limit  $R \rightarrow 0$  corresponds to the white-noise correlations of Refs. 4 and 10). In practice, the correlation function of surface inhomogeneities is not always Gaussian (see Refs. 12–14 and references therein). However, there are reasons to believe that the exact profile of the correlation function becomes important qualitatively only for large-scale roughness,  $R \gg L$ .<sup>15</sup>

Interplay between bulk and surface scattering can be described by two dimensionless parameters,  $t$  and  $u$ , the first of which characterizes the bulk scattering and the second—the correlation of surface roughness

$$t = \tau_b p_F^2 / m \hbar, \quad u = p_F^2 R^2 / \hbar^2 \sim R^2 / a^2 \geq 1, \quad (4)$$

where  $p_F \sim \hbar / a$  is the Fermi momentum,  $a$  is the atomic size.

In the case of phonon scattering, all temperature dependence of the surface-bulk interference contributions to conductivity enter solely via parameter  $t$ . At high temperatures  $T \gg \Theta_D$  the value of this parameter has the order of magnitude of<sup>16,17</sup>

$$t \sim \frac{\tau_b T_F}{\hbar} \sim \frac{T_F}{T} \gg 1, \quad \frac{t}{\sqrt{u}} = \frac{\tau_b p_F}{mR} \sim \frac{a T_F}{R T} \quad (5)$$

while at low temperatures  $T \ll \Theta_D$

$$t \sim \frac{\tau_b T_F}{\hbar} \sim \frac{T_F}{\Theta_D} \left( \frac{\Theta_D}{T} \right)^3 \gg 1, \quad \frac{t}{\sqrt{u}} = \frac{\tau_b p_F}{mR} \sim \frac{a T_F}{R \Theta_D} \left( \frac{\Theta_D}{T} \right)^3, \quad (6)$$

where  $\Theta_D$  is the Debye temperature. (There are experimental indications that  $\Theta_D$  in ultrathin films depends on film thickness).<sup>18</sup> At high temperatures, the ratio  $t/\sqrt{u}$  is large or small depending on whether the lateral size of surface inhomogeneities is smaller or larger than approximately  $10a$ . At low temperatures this ratio is always large with the exception of surfaces with extremely long-range inhomogeneities such

as in bent or nonuniformly stretched films with smooth surfaces. The transition between high- and low-temperature cases can be described by the usual extrapolation equations none of which are very reliable.

In the case of impurity scattering in the bulk, the parameter  $t$  is temperature independent,

$$t \sim \frac{\tau_b T_F}{\hbar} \sim \frac{a^2}{c\sigma}, \quad (7)$$

where  $c$  is the concentration of impurities and  $\sigma$  is the scattering cross-section.

In general, the non-Mathiesen's contribution to the collision time  $1/\tau_j^{(int)}$ , which describes the interference between bulk- and surface-scattering channels, can be defined as

$$\begin{aligned} \frac{1}{\tau_j^{(int)}(\mathbf{q})} &= \frac{1}{\tau_j^{(eff)}(\mathbf{q})} - \frac{1}{\tau_j^{(b)}(\mathbf{q})} \\ &- \lim_{t \rightarrow \infty} \sum_{j'=1}^S \int \frac{W_{jj'}(\mathbf{q}, \mathbf{q}')/\tau_{j'}^{(b)}(\mathbf{q}')}{[\epsilon_{j'}(\mathbf{q}') - T_F]^2/\hbar^2 + [1/2\tau_{j'}^{(b)}(\mathbf{q}')]^2} \\ &\times \frac{d\mathbf{q}'}{(2\pi\hbar)^2}. \end{aligned} \quad (8)$$

There are two major reasons why we cannot always use Eq. (1) directly for calculating the conductivity in ultrathin metal films. First, the observation of the full QSE effect in conductivity of metals is very difficult if not outright impossible. QSE in transport is associated with a saw-tooth dependence of the transport coefficients on the film thickness, Refs. 5 and 19. In metals, the scale of these saw teeth is atomic and there are very few observations of signs of such a saw-tooth dependence of the metal conductivity on  $L$ .<sup>20</sup> The reason is that the Fermi momentum in metals  $p_F$  is of the order of  $p_F \sim \hbar/a$ , where  $a$  is the atomic size. Then parameter  $p_F L/\hbar \sim L/a$  is usually large, the transport is quasiclassical, and the saw teeth too close to each other to be resolved. On top of that, the phonon collisions at not very low temperatures are rather robust,  $\tau_b \Delta \epsilon_j/\hbar \sim (a^2/L^2)(T_F/\Theta_D)$ , and can lead to smearing of QSE. This all means that Eq. (1) in metals should be replaced by a similar quasiclassical equation. This transition from quantum to quasiclassical transport is fairly straightforward and requires replacement of summation over the miniband index  $j$  by the integration over the continuous variable  $p_x$ ,  $\pi j\hbar/L \rightarrow p_x$ . Such a transition in the framework of helium Fermi liquids has already been suggested in Refs. 21 and 22; for further applications see also Ref. 23. As an additional benefit, the transition to the quasiclassical equations allows one to avoid dealing with atomistic peculiarities of the surface structure which lead to a reconstruction or even the destruction of the Fermi surface near the surface in the ultraquantum regime.<sup>24</sup>

The second reason for modification of Eq. (1) is the fact that this equation describes the two-channel collision time  $\tau^{(eff)}$  (i.e., the pole in the single-particle Green's function averaged over bulk and surface collisions) while the conductivity contains the effective transport time  $\tau_{tr}^{(eff)}$  which is defined via the diffusion pole in the proper response function

and, in our case, describes the single-particle diffusion/mobility or electric conductivity  $\sigma$ ,

$$\sigma = \frac{e^2 \tau_{tr}^{(eff)}}{m^2} \int \sum_{j'=1}^S \delta(\epsilon_j - \epsilon_F) q_j^2 \frac{q dq}{4\pi\hbar^2}, \quad q_j^2 = p_F^2 - \pi^2 \hbar^2/L^2. \quad (9)$$

Note, that our effective transport time  $\tau_{tr}^{(eff)}$  is not some phenomenological parameter but is an unambiguously defined quantity which describes the combined transport effects of the two-channel scattering. To get the transport time  $\tau_{tr}^{(eff)}$  and, therefore, the conductivity [Eq. (9)], one should solve the quantum transport equation with  $\tau_j^{(eff)}(\mathbf{q})$ , Eq. (1), in the kernel of collision operator. [For exact quantum definition of the transport time  $\tau_{tr}^{(eff)}$  via the irreducible bulk-scattering vertex and the surface-scattering probabilities  $W_{jj'}(\mathbf{q}, \mathbf{q}')$ , see Ref. 8]. This is a straightforward numerical task<sup>8</sup> only in the ultraquantum case which involves a relatively small number of minibands  $S$ ; in the quasiclassical limit with large  $S$  the corresponding transport equation involves an extremely large number of minibands and requires inversion of huge matrices. Even for small  $S$ , one needs detailed information on bulk-collision times  $\tau_j^{(b)}(\mathbf{q})$  for each miniband. Since we do not have such information about *bulk* collisions, we are forced to simplify the equations and work with constant  $\tau_j^{(b)}$ .

Analysis similar to Ref. 21 indicates that a reasonable quasiclassical approximation for the transport time  $\tau_{tr}^{(eff)}$  of Ref. 8 may be given by the quasiclassical equation

$$\frac{1}{\tau_{tr}^{(eff)}(\mathbf{p})} = \frac{1}{\tau_{tr}^b} + \frac{1}{\tau_b} \int \frac{W(\mathbf{p}, \mathbf{p}')(1 - \cos \gamma)}{[\epsilon(\mathbf{p}') - \mu]^2/\hbar^2 + 1/4\tau_b^2 (2\pi\hbar)^2} d\mathbf{p}' \quad (10)$$

where  $\gamma$  is the angle between vectors  $\mathbf{q}$  and  $\mathbf{q}'$ , the wall-scattering rate is

$$W(\mathbf{p}, \mathbf{p}') = \frac{4\pi}{L} \left( \frac{\ell R}{\hbar m} \right)^2 p_x^2 p_x'^2 \exp[-(\mathbf{q} - \mathbf{q}')^2 R^2/2\hbar^2], \quad (11)$$

and  $\tau_{tr}^b$  and  $\tau_b$  are *bulk* transport and collision times. Simultaneously, the quantum Eq. (9) acquires the simple Drude-type form

$$\sigma = \frac{e^2 n \tau_{tr}^{(eff)}}{m}. \quad (12)$$

Equation (10) becomes exact when the main contribution to lateral transport comes from the gliding electrons-electrons from the miniband with the smallest  $p_x$  when the bulk-collision time should be treated as  $\tau_1^b$ . In the limiting case of extremely large bulk-collision times, i.e., at very low temperatures, the convergence of the integral Eq. (10) is ensured by the quantum cutoff  $p_x = \pi\hbar/L$  rather than  $1/\tau_b$  in denominator.

What is lost in such transition from summation to integration is the presence of the quantum cutoff in transport that is responsible for capping the diverging contribution from gliding electrons to transport in high-quality low-temperature films. In sum in Eq. (1) the minimal component of momen-

tum perpendicular to the film is  $\pi\hbar/L$  and the sum is always finite. The quasiclassical integral Eq. (10), on the other hand, allows electrons to have zero normal component of momentum, i.e., allows existence of perfectly gliding electrons that do not collide with the surface and, therefore, contribute disproportionately to transport. Another result of the lack of quantum cutoff is that the dependence of the surface contribution to effective transport time on the film thickness becomes trivial. More complex dependencies of the transport coefficients on  $L$  in ultrathin high-quality films are almost invariably signs of the quantum cutoff and QSE.

At high temperatures  $T \gg \Theta_D$  the electron-phonon transport and collision times,  $\tau_{tr}^b$  and  $\tau_b$ , are roughly the same and differ from each other by an insignificant constant. A good estimate for  $\tau_{tr}^b$  and  $\tau_b$  can be obtained from the experimental data on bulk resistivity  $\rho$ ,<sup>17</sup>  $1/\tau_{tr}^b = ne^2\rho/m$ . Using the data for Cu,  $\rho(\theta_D) = 4.88 \times 10^{-8} \Omega \text{ m}$ ,  $n = 8.47 \times 10^{28} \text{ m}^{-3}$ , and  $\epsilon_F = 7 \text{ eV}$  and assuming that  $\tau_{tr}^b$  and  $\tau_b$  are the same, one gets  $t \approx 173 (\Theta_D/T)$ . Similar estimate for Ag,  $n = 5.86$

$\times 10^{28} \text{ m}^{-3}$ ,  $\rho(\theta_D) = 3.5 \times 10^{-8} \Omega \text{ m}$ ,  $\epsilon_F = 5.49 \text{ eV}$  yields  $t \approx 273 (\Theta_D/T)$  meaning that cases  $t$  is relatively large for both metals. At low temperatures  $T \ll \Theta_D$  bulk-transport and -collision times are markedly different,  $\tau_{tr}^b \sim (\Theta_D/T)^2 \tau_b \gg \tau_b$ . In the case of impurity scattering the difference between  $\tau_{tr}^b$  and  $\tau_b$  is less pronounced.

### III. EFFECTIVE TRANSPORT TIME

In this section we give simple estimates for the effective transport time [Eq. (10)]. Introducing new variables as

$$p_x = p_F \cos \theta, \quad q = p_F \sin \theta, \quad p'_x = xp_F \cos \phi,$$

$$q' = xp_F \sin \phi, \quad n = p_F^3/3\pi^2\hbar^3 \quad (13)$$

one can reduce the effective transport time [Eq. (10)] to a dimensionless integral

$$\frac{1}{\tau_{tr}^{eff}} = \frac{1}{\tau_{tr}^b} + \frac{12T_F \ell^2 R^2 n}{\pi\hbar L} \frac{1}{t} \int_0^\pi d\theta \cos^2 \theta \int_0^\infty x^4 dx \int_0^\pi d\phi \int_0^{2\pi} d\gamma \times \frac{\cos^2 \phi \sin \phi e^{-u/2(\sin^2 \theta + x^2 \sin^2 \phi - 2x \sin \theta \sin \phi \cos \gamma)} [1 - \cos \gamma]}{\left[ (x^2 - 1)^2 + \frac{1}{t^2} \right]}. \quad (14)$$

After integration over  $d\gamma$ , the transport time reduces to

$$\begin{aligned} \frac{1}{\tau_{tr}^{eff}} &= \frac{1}{\tau_{tr}^b} + \frac{T_F \ell^2}{\hbar L \lambda_F} U(u, t), \\ U(u, t) &= \frac{16u}{\pi} \int_0^\pi d\theta \cos^2 \theta e^{-u/2(\sin^2 \theta + 1)} \int_0^\infty dy y^4 e^{-u/2(y^2 - 1)} \\ &\quad \times [I_0(uy \sin \theta) - I_1(uy \sin \theta)] F_1(y, t), \\ F(y, t) &= \frac{1}{t} \int_0^\pi d\phi \frac{\cos^2 \phi}{[(y^2 - \sin^2 \phi)^2 + \sin^4 \phi/t^2]}, \quad (15) \end{aligned}$$

where we replaced  $x$  by  $y = x \sin \phi$ .

All information about quasiclassical interference between surface and bulk scattering is contained in the function  $U(u, t) - U_0(u)$ , where  $U_0(u) = U(u, t \rightarrow \infty)$ . This function is plotted in Fig. 1 as a function of  $t$  for three different values of  $u$ ,  $u = 1; 10; 10$ , while the function  $U_0(u)$  is plotted in Fig. 2. It is clear from the plot that the interference contribution decreases with increasing  $t$  and with increasing correlation radius of surface roughness  $R$  (with increasing  $u$ ). For high-quality films with large bulk mean free paths for which  $t$  is large,  $t \gg 1$ , it is possible to obtain a relatively simple semianalytical description of  $U(u, t)$  as an expansion in  $1/t$ . Note that  $U(u, t)$  is not a regular function of  $1/t$  and the expansion is, strictly speaking, in the powers of  $1/\sqrt{t}$ .

Integrals in Eqs. (14) and (15) are rather cumbersome. To better understand the results below one should keep in mind that at large  $t$  and  $u$  the integrand is a product of two peaks one of which is a function of  $t$  and the other—a function of  $u$ .

The first peak is explained by a relatively large value of the electron-phonon collision time  $\tau_b$  in clean metals at not very high temperatures and, therefore, by the large value of the dimensionless parameter  $t \gg 1$ . Function  $F(y, t \rightarrow \infty)$  has singularities at  $y \rightarrow 0$  and  $y \rightarrow 1$ . The former singularity is not dangerous because of the factor  $y^4$  in the integrand. The latter one is eliminated by the factor  $1/t$  in front of the integral. The peak in  $y^4 F(0 < y < 1, t \rightarrow \infty)$  is asymmetric and is rather broad. From the physics standpoint, this asymmetry reflects the higher contribution to lateral transport from the gliding electrons with momenta almost parallel to the film surface. Function  $y^4 F(0 < y < 1, t \rightarrow \infty)$  gradually increases when  $y$  increases from 0 to 1 and rapidly drops almost to zero again when  $y$  start approaching 1. At large  $t$  the shape and parameters of this peak practically do not depend on  $t$  except for a very narrow region near 1 in which  $1 - y^2 \sim 1/t$ . At  $y > 1$ , function  $F(y, t \rightarrow \infty)$  remains small.

In contrast to this, the peak of the integrand as a function of  $y$  at  $u \gg 1$  (or, more precisely, at  $\sqrt{u} \gg 1$ ) represents a narrow peak of the width  $1/\sqrt{u}$ . At  $\sqrt{u} \gg 1$  the integrand in Eq. (15) can be simplified using the asymptotic expressions for the Bessel functions,



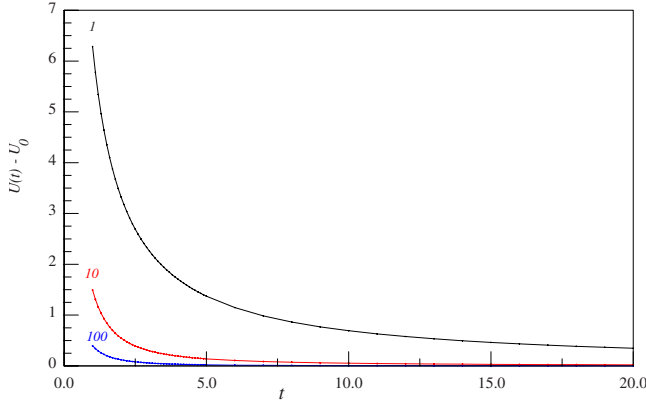


FIG. 1. (Color online) The interference contribution to the function  $U(u,t)$ , Eq. (15). The plotted function is  $U(u,t) - U_0(u) \equiv U(u,t) - U(u,t \rightarrow \infty)$  as a function of  $t$  at three fixed values of  $u$ ,  $u=1$ ; 10; 100. The curves are marked accordingly.

$$I_{0,1}(z \gg 1) \sim e^z / \sqrt{2\pi z}, \quad (16)$$

which makes the integrand look like a Gaussian function,

$$e^{-u/2(y - \sin \theta)^2}, \quad (17)$$

and in the limit  $u \rightarrow \infty$ —almost like a  $\delta$  function,

$$\begin{aligned} & y^4 e^{-u/2(y^2-1)} [I_0(uy \sin \theta) - I_1(uy \sin \theta)] \\ & \rightarrow \frac{1}{u} y^3 e^{u(\sin^2 \theta + 1)/2} \delta(y - \sin \theta). \end{aligned} \quad (18)$$

This peak in the integrand at  $\sqrt{u} \sim R/a \gg 1$  is explained by a small momentum transfer  $\delta q \sim \hbar/R$  in scattering by smooth inhomogeneities with large lateral size  $R$ .

Integration over  $d\phi$  in Eq. (15) yields the following expression for  $F(y,t)$ :

$$F(y,t) = \frac{\pi}{\sqrt{2}y^3} \frac{1/t}{\left[ \sqrt{(y^2-1)^2 + \frac{1}{t^2} + (y^2-1)} \right]^{1/2}}. \quad (19)$$

The singularity at  $y=0$  is eliminated by the extra factor  $y^4$  [or, rather,  $y^{7/2}$  because of the Bessel functions Eq. (16)] in the integrand in Eq. (15). Everywhere between  $0 < y < 1$ , except for points very close to  $y=1$ ,

$$F(0 < y < 1, t \rightarrow \infty) \simeq F_0(y) = \frac{\pi}{2y^3} \sqrt{1-y^2}. \quad (20)$$

Corrections to this equation are of the order of  $1/t^2$ ,

$$\frac{\pi}{8t^2 y^3 (1-y^2)^{3/2}}, \quad (21)$$

except for a very narrow region  $y \rightarrow 1$ .

At  $y > 1$ , but again not very close to  $y=1$ , the main term in the function  $F(y,t \gg 1)$  is of the order of  $1/t$  and is, therefore much smaller than Eq. (20)

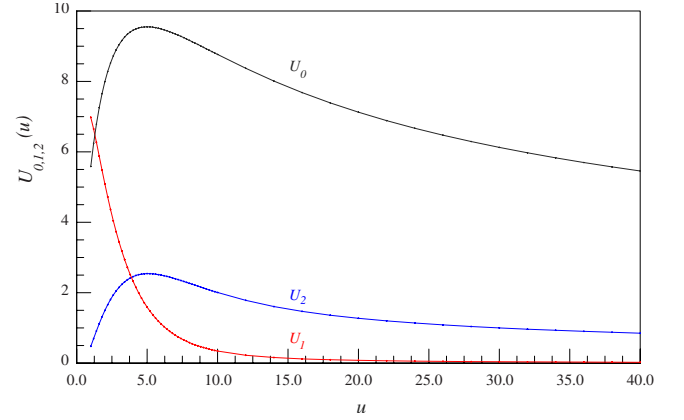


FIG. 2. (Color online) Functions  $U_{0,1,2}(u)$ , Eq. (25). The curves are marked accordingly.

$$F_1(y > 1, t \gg 1) \simeq F_1(y) = \frac{1}{t} \frac{\pi}{2y^3} \frac{1}{\sqrt{y^2-1}}. \quad (22)$$

The contribution from this region to the integral over  $dy$  is usually small, especially at  $u \gg 1$  since the corresponding integral is also exponentially small in  $u$ .

Function  $U(u,t \gg 1)$  is not an analytical function of  $1/t$ . Close to the point  $y=1$ , i.e., when  $1/t \gg |1-y^2|$ , function  $F_1(y \rightarrow 1, t \gg 1)$  behaves as  $1/\sqrt{t}$  on both sides of  $y=1$ ,

$$F(y \rightarrow 1, t \gg 1) \rightarrow \frac{\pi}{\sqrt{2t}}. \quad (23)$$

Since the width of this region is approximately  $1/t$ , its contribution to the integral is of the order of  $1/t^{3/2}$ . To find this nonanalytical contribution one can keep only the main term in  $(y-1)$  in  $F(y,t)$ ,

$$\tilde{F}(y < 1, t) = \frac{\pi}{\sqrt{2}} \frac{1/t}{\left[ \sqrt{4(y-1)^2 + \frac{1}{t^2} + 2(y-1)} \right]^{1/2}}, \quad (24)$$

and put  $y=1$  into all coefficients in front of  $F$ . The remaining integral,

$$\int_0^1 \tilde{F} dy,$$

can be evaluated exactly. The main nonanalytical contribution from this term is  $1/(3\sqrt{2}t^{3/2})$ . To get the nonanalytical contribution from the region  $y > 1$ , one should cutoff the corresponding integral at some large value  $A$ . The exact value of the cutoff  $A$  is, of course, irrelevant for the nonanalytical contribution from the area close to  $y=1$  which turns out to be  $-1/(3\sqrt{2}t^{3/2})$ . Therefore, the term  $1/t^{3/2}$  disappears from the function  $U(u,t \gg 1)$  and the first nonregular term in the expansion of the function  $F$  in  $1/t$  has the order  $1/t^{5/2}$ . The latter term is not important in our context.

Summarizing, at  $t \gg 1$  the leading terms in the expansion of  $U(u,t \gg 1)$  in  $1/t$  are

$$U(t \gg 1, u) \simeq U_0(u) + \frac{1}{t}U_1(u) + \frac{1}{t^2}U_2(u) \quad (25)$$

with  $U_0(u)$  coming from Eq. (20),  $U_1(u)$  coming from Eq. (22), and  $U_2(u)$ —from Eq. (21). Functions  $U_0(u)$ ,  $U_1(u)$ , and  $U_2(u)$  are plotted in Fig. 2.

The analytical expression for  $U_0(u)$  is

$$\begin{aligned} U(u, t \rightarrow \infty) &\equiv U_0(u) \\ &= 16u \int_0^\pi d\theta \cos^2 \theta e^{-u/2(\sin^2 \theta + 1)} \int_0^1 \sqrt{1-y^2} y dy e^{-u/2(y^2-1)} \\ &\quad \times [I_0(uy \sin \theta) - I_1(uy \sin \theta)]. \end{aligned} \quad (26)$$

This function can be simplified at  $u \gg 1$  using Eq. (18)

$$\begin{aligned} U_0(u \gg 1) &\simeq 16\sqrt{2\pi u} \int_0^\pi d\theta \sin \theta |\cos^3 \theta| \\ &\quad \times \frac{[I_0(u \sin^2 \theta) - I_1(u \sin^2 \theta)]}{e^{u \sin^2 \theta}} \\ &= 16\sqrt{\frac{2\pi}{u}}. \end{aligned} \quad (27)$$

The result indicates that when the lateral size of surface inhomogeneities  $R$  becomes bigger and the walls smoother, the wall-driven transport time increases proportionally to  $1/R$ . This term gives the pure surface contribution to transport.

The next terms in the expansion in  $1/t$  are responsible for the surface-bulk interference in transport beyond the Mathiessen's rule. The first such term is

$$\begin{aligned} U_1(u) &= 8u \int_0^\pi d\theta \cos^2 \theta e^{-u/2(\sin^2 \theta + 1)} \\ &\quad \times \int_1^\infty dy \frac{y}{\sqrt{y^2-1}} e^{-u/2(y^2-1)} \\ &\quad \times [I_0(uy \sin \theta) - I_1(uy \sin \theta)]. \end{aligned} \quad (28)$$

At large  $u$  this function behaves as  $1/u^{3/2}$ . More accurately,

$$\begin{aligned} U_1(u \gg 1) &\simeq \frac{8u}{2\sqrt{2\pi}} \int_0^\pi d\theta \cos^2 \theta e^{-u \sin^2 \theta/2} \\ &\quad \times \int_1^\infty dy \frac{y}{\sqrt{y^2-1}} \frac{e^{-uy^2/2} e^{yu \sin \theta}}{(yu \sin \theta)^{3/2}} \\ &\simeq \frac{10}{u^{3/2}} \sqrt{\frac{2}{\pi}} \end{aligned} \quad (29)$$

(the last equation is a result of a numerical evaluation rather than of the exact analytical calculation of the integral). This also means that at  $u \gg 1$

$$U_1/U_0 \rightarrow 5/(8\pi u) \quad (30)$$

and the contribution from  $1/t$  becomes less and less significant with increasing lateral size of surface inhomogeneities  $R$ .

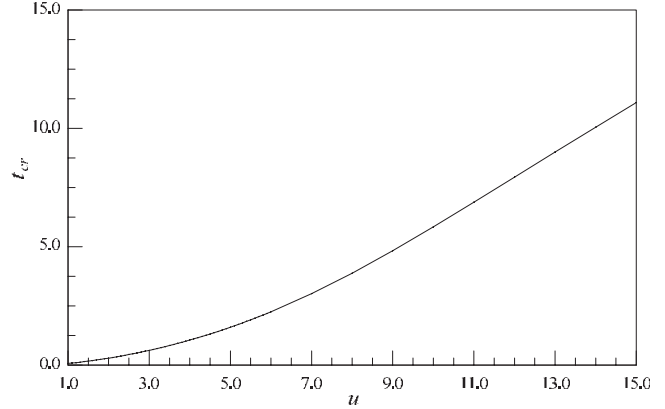


FIG. 3. Function  $t_{cr}(u)$ , Eq. (32), which determines the crossover from  $1/t^2$  to  $1/t$  dependence of the surface-bulk interference contribution to the effective scattering time.

The computation of  $U_2(u)$  is more cumbersome. This function comes from the integration over  $dy$  from 0 to 1. To get this function, one should subtract from the correspondent integral not only the zeroth-order term  $F_0$  but also the terms that yield the  $1/t^{3/2}$  contribution

$$\begin{aligned} U_2 &= 16u \lim_{t \rightarrow \infty} t^2 \int_0^\pi d\theta \cos^2 \theta e^{-u/2(\sin^2 \theta + 1)} \int_0^1 dy \\ &\quad \times \left\{ f(y)(F - F_0 - \tilde{F} + \tilde{F}_0) + [f(y) - f(1)](\tilde{F} - \tilde{F}_0) \right. \\ &\quad \left. + f(1) \left( \tilde{F} - \tilde{F}_0 - \frac{1}{3\sqrt{2}t^{3/2}} \right) \right\}, \\ f(y) &= y^4 e^{-uy^2/2} [I_0(uy \sin \theta) - I_1(uy \sin \theta)], \\ \tilde{F}_0 &= \frac{\sqrt{2\pi}}{y^3} \sqrt{1-y}. \end{aligned} \quad (31)$$

As it is clear from Fig. 2,  $U_2(u) \gg U_1(u)$  at  $u \gg 1$ . The reason is quite simple. At large values of  $u$  the coefficients in front of  $F$  in the integral over  $dy$  form an almost Gaussian peak around some value of  $y < 1$ . Therefore,  $U_2(u)$ , which originates from the integral over  $dy$  from 0 to 1, always dominates at  $u \gg 1$  over  $U_1(u)$ , which originates from the integral from 1 to  $\infty$ . As a result, the term  $U_2(u)/t^2$  in the expansion (25) of  $U(u, t \gg 1)$  over  $1/t$  can remain much larger than  $U_1(u)/t$  even at large values of  $t$ . The crossover from  $U_2(u)/t^2$  to the asymptotic behavior  $U_1(u)/t$  occurs only when  $t$  exceeds some critical value  $t_{cr}$ ,

$$t_{cr}(u) = U_2(u)/U_1(u). \quad (32)$$

Function  $t_c(u)$  is plotted in Fig. 3. At relatively small values of  $u$  (for practical purposes, at  $u \leq 10$ ),  $t_c$  is quadratic in  $u$ ,  $t_{cr} \approx 0.1u^2$ . At larger values of  $u$  (numerically, at  $u \geq 15$ ),  $t_c$  is linear in  $u$ ,  $t_c \approx u$ . We can prove from analyzing the asymptotic behavior of  $U_2(u)$  and  $U_1(u)$  at  $u \gg 1$  that  $U_2(u) \propto 1/u^{1/2}$  and  $U_1(u) \propto 1/u^{3/2}$  and, therefore,  $t_c$  is indeed linear in  $u$ . However, we cannot prove that the proportionality coefficient is exactly 1. Numerically, this coefficient is approxi-

mately 0.99 though the accuracy of computation for Eq. (31) is limited by the presence of nonanalytical term  $1/t^{5/2}$ . In the end, the assumption  $t_c(u \gg 1) = u$  is sufficiently good for any potential comparison with experiment.

Summarizing, in high-quality films with  $t, u \gg 1$

$$U(t \gg 1, u \gg 1) \simeq \frac{10}{\pi} \sqrt{\frac{2\pi}{u}} \left( \frac{8\pi}{5} + \frac{1}{tu} + \frac{1}{t^2} \right) \quad (33)$$

or in normal variables

$$\frac{1}{\tau_{tr}^{eff}} \simeq \frac{1}{\tau_{tr}^b} + \frac{10\sqrt{2}}{\sqrt{\pi}} \frac{T_F}{p_F \lambda_F R L} \frac{\ell^2}{R} \left( \frac{8\pi}{5} + \frac{\hbar}{2\tau_b T_F} \frac{\lambda_F^2}{R^2} + \frac{\lambda_F^2 m}{2\tau_b^2 T_F} \right). \quad (34)$$

This simple equation describes the asymptotic behavior of the wall contribution to conductivity of films [Eq. (15)] in the classical approximation. The crossover from  $1/\tau_b$  to  $1/\tau_b^2$  behavior of the interference term occurs at  $R^2 \sim a\mathcal{L}_b$ .

It could be instructive to compare the pure wall term in Eq. (34) with the Fuchs-Sondheimer result for the resistivity  $\rho$ ,

$$\rho = \rho_b \left[ 1 + \frac{3\mathcal{L}_b}{8L} (1-p) \right]. \quad (35)$$

The comparison yields the following expression for the specularity coefficient  $0 \leq p \leq 1$ :

$$p = 1 - \frac{64}{3} \sqrt{2\pi} \frac{\ell^2}{\lambda_F R} \quad (36)$$

meaning that the Fuchs boundary condition can emulate scattering by rough surfaces only for a very small amplitude of roughness,  $\ell^2 \ll \lambda_F R$ . This restriction is noticeably stronger than restriction on our approach<sup>7</sup>  $\ell \ll R, L$ . Of course, the Fuchs-Sondheimer Eq. (35) does not contain the interference terms which represent the main thrust of this paper. Note that, in principle, the Fuchs boundary condition, which assumes partial accommodation by the perfect flat walls, does not have to emulate the results of locally specular scattering by rough walls for which the mean free path is established by the randomization of lateral momentum due to a series of reflections from randomly directed walls.

#### IV. ACCURACY OF THE RESULTS

Before discussing our results, we would like to comment on the accuracy of our predictions and on the ways for improvements. Though some of these potential improvements could seem rather straightforward, the others might require us to introduce new parameters, which, in turn, could make the results useless for any meaningful comparison with experiment. Below we will list some of the restrictions on the accuracy of our results and describe the ways of lifting these restrictions.

##### A. Accuracy of the main equations

Our results are based on a thorough diagrammatic derivation of the transport equation in films with bulk and rough-

ness scattering channels in Ref. 8. As it is shown in Ref. 8, the effective relaxation time  $1/\tau_j^{(eff)}(\mathbf{q})$  reduces after averaging over surface roughness and bulk scattering to two diagrams for the self-energy function. The first one leads directly to Eq. (1) while the second one is disregarded following Ref. 8. This is a common approximation used, in different forms, in most of the Green's function based transport derivations (see, e.g., Refs. 10 and 25 and references therein). This approximation is well justified when the bulk interaction has a short range which is usually the case for impurity scattering. For phonon scattering it might not work as well at very low temperatures.

In principle, we can add this disregarded second diagram to the equation for the pole of the single-particle Green's function Eq. (1). However this would lead to a loss of transparency of the results and make any meaningful comparison with experiment virtually impossible: this diagram contains integrals with the full irreducible bulk vertex function, which is unknown and does not reduce to observables.

A somewhat more worrisome is the heuristic transition from the quantum Eq. (1) for the relaxation time to the quasiclassical Eq. (10) for the transport time. This transition allowed us avoid inverting huge matrices stemming from the transport equation and get the quasiclassical results in a very compact analytical form. This is justified when the dominant contribution to transport comes from gliding electrons which are contained in the lowest quantum miniband and when the pure wall scattering dominates over the interference terms. We plan to revisit this issue in more detail later on.

##### B. Non-Gaussian correlations

The above results assume that the correlation function of surface roughness has a Gaussian form, Eqs. (1)–(3). Though the Gaussian correlations are practically universally used for theoretical description of rough surfaces, there is experimental evidence the correlations are sometimes non-Gaussian (see, e.g., Refs. 12–14). The difference between transport properties of *quantized* films with various types of surface correlations could be quite noticeable, especially for relatively smooth surfaces with  $R \gg a$  which can exhibit, depending on the type of the correlation function, a new type of quantum size effect, Ref. 15. In the case of quasiclassical transport the difference is less striking and is easy to analyze. For example, the change in the correlation function leads to a replacement of the Gaussian factor in the integrand  $W$ , Eq. (11), by some other exponential or power-law function, which properly reflects the correlations, and results in a different power in the dependence  $U(u)$ . Numerically this is a straightforward matter. The semianalytical comparison between different roughness profiles will be done in a separate paper.

##### C. Surface-driven deformations

In our description of transport we assumed that the main transport effect of surface roughness is the scattering by surface inhomogeneities that reflect randomness in the position and direction of the surface. As a result, the transport parameters depend solely on the geometry of the surface, i.e., the

correlation function of surface roughness, and do not take into account the change in electron or phonon properties near the surface. Of course, the proximity to the surface leads to deformations inside the film, which affect the electron properties via the deformation potential. The deformation potential near surface inhomogeneities, especially near the ones with large curvature, changes the scattering parameters and makes the effective averaged cross-section different from the purely geometry-driven one. We discussed the ways to incorporate this effect into our formalism in Ref. 7. Essentially, this is equivalent to the replacement of the scattering probability Eq. (11) by an effective function with similar symmetry. This resembles the description of transport in systems with bulk impurities in which the impurity-scattering potential  $U(\mathbf{r})$  is replaced by the effective  $T$ -matrix  $T(\mathbf{p}, \mathbf{p}')$ . Though this is the right way of dealing with the complications stemming from the surface-driven deformations, the *experimental* implications are not very appealing. The correlation function of surface roughness  $\zeta(\mathbf{q})$  can be measured directly by scattering experiments, scanning surface microscopy, etc. This information is sufficient for direct application of our results without any unknown fitting parameters. If, on the other hand, the deformation potential near the surface is strong, one is forced to treat  $W(\mathbf{p}, \mathbf{p}')$  as an effective average scattering cross-section. This inevitably leads to an appearance of fitting parameters and makes the results more ambiguous.

Another issue is the softening of phonon spectrum and, therefore, lowering of the Debye temperature near the surface.<sup>18</sup> When this effect is strong, the “bulk” scattering parameters that enter our non-Mathiesen’s terms may differ considerably from their true bulk values.

#### D. Quantum size effect

One of the main features of our results is the  $1/L$  dependence of the wall contribution to the effective transport time  $1/\tau_{tr}^{(eff)}$  on the film thickness which is consistent with the quasiclassical Fuchs-Sondheimer theory. In ultraclean films at very low temperatures, i.e., at  $t \rightarrow \infty$ , the contribution from the gliding electrons should be cutoff not by  $i/t$  in the pole of the integrand, but by the quantum cutoff,  $p_x, p'_x > \pi\hbar/L$ ,

$$\frac{1/\tau_b}{[\epsilon(\mathbf{p}') - \mu]^2/\hbar^2 + 1/4\tau_b^2} \rightarrow 2\pi\delta[\epsilon(\mathbf{p}) - \mu], \quad (37)$$

$$\begin{aligned} \frac{1}{\tau_{tr}^{(eff)}} &= \frac{1}{\tau_b} + 2\pi \int_{p'_x > \pi\hbar/L} W(\mathbf{p}_F, \mathbf{p}') \\ &\times \delta[\epsilon(\mathbf{p}) - \epsilon_F] \frac{(1 - \cos \gamma) d\mathbf{p}'}{(2\pi\hbar)^3}. \end{aligned} \quad (38)$$

Apart from ensuring the low-temperature cutoff, Eq. (38) also makes the dependence of the lateral conductivity  $\sigma$  on the film thickness  $L$  much more complicated than in Sec. III leading, for example, to  $1/L^2$  (Refs. 7, 15, and 23) or  $1/L^3$  dependence.<sup>7,9</sup> This more complicated wall contribution to the effective transport time  $1/\tau_{tr}^{(eff)}$  than  $1/L$  in experiment might be a direct sign of quantum size effects in transport.

An even more accurate account of the quantum size effect would require us to return to summation, Eq. (1), instead of integration and to a saw-tooth dependence of the conductivity on the film thickness  $L$  which is similar to the one of Ref. 8 and is a common feature of QSE in films irrespective of the scattering channel.<sup>5,7,19</sup> However, in metals the width of these saw teeth is about atomic size  $a$  and the observation of this type of dependence  $\sigma(L)$  highly unlikely. We plan to study the effect of the quantum cutoff on the quasiclassical effective transport time separately.

#### E. Momentum dependence of the bulk relaxation time and quantization of phonons

The discussion above ignores the quantization of phonons in ultrathin films and, even more importantly, the momentum dependence of the bulk relaxation time  $\tau_b(p_x, \mathbf{q})$  in Eq. (1). Not much is known about this function that can be useful in our context. Though one can easily write the formal expressions for  $\tau_b(\mathbf{p})$  (see, for example, Refs. 16 and 17 and numerous other publications), these expressions do not reduce to a set of observables which are independently known from experiment. In the end, any attempt to make our results more accurate by introducing the dependence  $\tau_b(\mathbf{p})$  into the calculations would leave us with a large additional set of fitting parameters that would only obscure our understanding of surface contribution to transport in films.

The only real improvement could be achieved for ultrathin films at very low temperatures for which we should replace the averaged bulk experimental value  $\tau_b$  used above by the corresponding constant for the gliding electrons  $\tau_b(\pi\hbar/L, \mathbf{q}_F)$ —when this constant is known experimentally. The next step in the same directions could be the use of quantized—ultimately, two dimensional—phonons. This will lead to an obvious change in the temperature dependence of the results.

#### F. Localization and related quantum interference phenomena

Above we deliberately ignored the roughness-driven localization of electrons. The localization length in quasi-two-dimensional films with weak roughness is exponentially large and can manifest themselves only for the ultrathin films. Localization corrections within our formalism are discussed in detail in the second of Ref. 7 which also contains references to earlier publications on localization and quantum interference effects associated with the surface disorder.

## V. DISCUSSION

The most interesting part of our results for the quasiclassical interference between bulk- and surface-scattering channels in electron transport in thin films is, probably, our simple asymptotic expression (34) for high quality films with large bulk free path  $\mathcal{L}_b$  (i.e., large  $t$ ) and large lateral size of surface inhomogeneities  $R$  (i.e., large  $u$ ). We do not know of other publications with such simple and easily verifiable result. This result includes a crossover between two different asymptotic behaviors of the resistivity at  $\mathcal{L}_b \sim R^2/a$ . Irrespective of the bulk-scattering channel, the crossover in the



interference part of the resistivity can be observed as a change in its dependence on the correlation length (lateral size) of surface inhomogeneities  $R$  from  $1/R^3$  to  $1/R$ . Experimentally this crossover can manifest itself also as a change in the temperature (phonon-scattering) or concentration (impurity-scattering) dependencies of the resistivity. Note, however, that when the  $1/ut$  term in the interference contribution [Eqs. (33) and (34)] dominates over the  $1/t^2$  term, the temperature/concentration dependence of the interference contribution is exactly the same as for the bulk term and the only distinguishing feature of the interference contribution is its  $1/R^3$  dependence on  $R$ . Of course, when  $1/t^2$  term dominates, the temperature/concentration dependence of the interference contribution is quite distinct from the main surface term.

Despite many decades of experiments on conductivity of ultrathin films, there are very few data sets on the functional behavior of the interference between bulk and roughness-driven scattering. The usual experimental difficulties are ensuring that roughness is the main boundary scattering channel and maintaining the same surface roughness while manipulating the bulk properties. Currently, we are aware of only one group which accompanies the measurements of the interplay between electron-phonon and roughness scattering channels as a function of temperature by the simultaneous analysis of surface roughness.<sup>14,26</sup>

It is instructive to compare our semianalytical quasiclassical results with previous quantum computations which explicitly include QSE.<sup>4,5,8,10</sup> Reference 4 does not contain any explicit equations for the interference terms that can be compared with our results, especially in the quasiclassical regime. The authors of Ref. 5 were not interested in the interference terms and considered bulk and roughness scattering as two independent additive channels. Reference 10 also does not contain any explicit information about the interference terms except for mentioning that these contributions seem to be smaller than the pure wall or bulk terms. In addition, Refs. 4, 5, and 10 use the  $\delta$ -type (white-noise) approximation for the surface roughness and, therefore, would not be able to see the crossover between interference regimes even if there were analytical results for the surface-bulk interference.

In our earlier computations of Ref. 8 we characterized the interference term by a dimensionless parameter  $\chi$  which described the ratio of pure-wall and bulk-wall interference contributions to the effective relaxation (or transport) time or the resistivity Eq. (12),

$$\chi = 1 + \frac{\tau^w}{\tau^{int}}.$$

In our notations,

$$\chi = \frac{U(t, u)}{U(t \rightarrow \infty, u)}.$$

For high-quality clean films as in Eq. (33), this ratio acquires the simplest form,

$$\chi = 1 + \frac{5}{8\pi} \left( \frac{1}{tu} + \frac{1}{t^2} \right) \quad (39)$$

and the correction to the limiting value  $\chi=1$  is positive.

The result in Eq. (39) can be compared with the QSE dependence of  $\chi$  on the bulk free path  $\mathcal{L}_b$ ,  $\chi(p_0\mathcal{L}_b)$ , in Ref. 8 ( $p_0\mathcal{L}_b$  in Ref. 8 is equivalent to our  $2t$ ). As it is clear from figures in Ref. 8, the correction to the limiting value  $\chi=1$  can be positive or negative, depending on the number of quantum minibands involved though it tends to become more negative with an increase in the number of minibands (increase in film thickness). Also, the deviation of  $\chi$  from 1 in quantum case seems to increase with increasing  $R$  (i.e., with increasing  $u$ ). It is not clear why the results of the same approach in quantum and classical limits are so different. One of the reasons could be the above-mentioned heuristic transition from Eq. (1) to Eq. (10) in which we averaged the transport time over all minibands while structuring the result closer to discrete equations of Ref. 8 for the lowest minibands which contain the gliding electrons.

In experiments<sup>14,26</sup> the correction to  $\chi=1$  seems to be negative (the corresponding term in resistivity  $\Delta\rho$  decreases with increasing temperature). Though it is impossible to make a quantitative comparison with our results, qualitatively we tend to interpret these results as an experimental manifestation of QSE. There is one caveat. The experimental values of  $\rho(T)$  are very close to the pure bulk values  $\rho_b(T)$  and the functional behavior of both functions is identical. One cannot discount the possibility that the surface-driven softening of the phonon modes and the renormalization of the Debye temperature should require the use of a renormalized function  $\tilde{\rho}_b(T)$  rather than the true bulk function  $\rho_b(T)$  as the basis for extracting  $\Delta\rho$  from experiment.<sup>18</sup> If the mode softening is sufficiently strong, the extracted values of  $\Delta\rho$  will actually increase with increasing temperature and exhibit the temperature dependence consistent with our  $1/t$  dependence of the interference terms.

The dependence on the film thickness  $L$ ,  $1/\tau^{int}(L)$ , in Ref. 8 starts, if one disregards the inevitable QSE saw teeth, from the ultraquantum form  $1/L^6$  and shifts to  $1/L^3$  in thicker films and finally to  $1/L$  in thick films with dominant higher minibands. This behavior is consistent with our current results which yield the  $1/L$  dependence without the quantum cutoff and higher powers when this cutoff becomes essential, Eq. (38). This also tells us that more often than not one should not expect a clear-cut power law in experimental dependence of resistivity on  $1/L$ . Accordingly, experimental data on the dependence of the resistivity on  $1/L$  are inconclusive. One of additional artifacts is the potential presence of grain boundaries that can distort the roughness contribution if the films are not properly annealed as it has been recently demonstrated in Ref. 27. Some of the recent experimental data have been summarized in Ref. 26. This summary also does not lead to any definite conclusion on the power in the dependence of resistivity on  $1/L$ . Recent experimental results of Ref. 28 yield the dependence  $1/L^{1.2}$  which is consistent with our results though the number of experimental points is relatively small to make a definite conclusion. As it was mentioned before, a higher power of  $1/L$  in experimen-

tal data on the dependence of resistivity on film thickness for ultrathin films should be considered as a sign of QSE in transport at least in the form of the quantum cutoff.

In summary, we analyzed classical interference between bulk- and surface-scattering processes in electron transport in thin films. The results acquire a very simple analytical form for high-quality films with large bulk mean free paths  $\mathcal{L}_b$  and

large lateral size of surface inhomogeneities  $R$ . There is a marked crossover between two different interference regimes when  $\mathcal{L}_b \sim R^2/a$ . This crossover should manifest itself in change in the temperature dependence of the interference contribution when the electron-phonon scattering is the main bulk-scattering channel or in change in the dependence on impurity concentration.

- 
- <sup>1</sup>E. H. Sondheimer, *Adv. Phys.* **1**, 1 (1952); J. R. Sambles, *Thin Solid Films* **106**, 321 (1983); K. Fuchs, *Proc. Cambridge Philos. Soc.* **34**, 100 (1938).
- <sup>2</sup>Y. Namba, *Jpn. J. Appl. Phys.* **9**, 1326 (1970).
- <sup>3</sup>J. J. Plombon, E. Andideh, V. M. Bubin, and J. Maiz, *Appl. Phys. Lett.* **89**, 113124 (2006).
- <sup>4</sup>Z. Tešanović, M. V. Jarić, and S. Maekawa, *Phys. Rev. Lett.* **57**, 2760 (1986); Z. Tesaonovic, *J. Phys. C* **20**, L829 (1987).
- <sup>5</sup>N. Trivedi and N. W. Ashcroft, *Phys. Rev. B* **38**, 12298 (1988).
- <sup>6</sup>A. E. Meyerovich and S. Stepaniants, *Phys. Rev. Lett.* **73**, 316 (1994).
- <sup>7</sup>A. E. Meyerovich and A. Stepaniants, *Phys. Rev. B* **58**, 13242 (1998); **60**, 9129 (1999).
- <sup>8</sup>A. E. Meyerovich and A. Stepaniants, *J. Phys.: Condens. Matter* **12**, 5575 (2000).
- <sup>9</sup>G. Fishman and D. Calecki, *Phys. Rev. Lett.* **62**, 1302 (1989); *Phys. Rev. B* **43**, 11581 (1991).
- <sup>10</sup>L. Sheng, D. Y. Xing, and Z. D. Wang, *Phys. Rev. B* **51**, 7325 (1995).
- <sup>11</sup>R. C. Munoz, G. Vidal, G. Kremer, L. Moraga, and C. Arenas, *J. Phys.: Condens. Matter* **11**, L299 (1999).
- <sup>12</sup>J. A. Ogilvy, *Theory of Wave Scattering from Random Surfaces* (Adam Hilger, Bristol, 1991).
- <sup>13</sup>R. M. Feenstra, D. A. Collins, D. Z.-Y. Ting, M. W. Wang, and T. C. McGill, *Phys. Rev. Lett.* **72**, 2749 (1994).
- <sup>14</sup>R. C. Munoz, G. Vidal, G. Kremer, L. Moraga, C. Arenas, and A. Concha, *J. Phys.: Condens. Matter* **12**, 2903 (2000).
- <sup>15</sup>A. E. Meyerovich and I. V. Ponomarev, *Phys. Rev. B* **65**, 155413 (2002); Y. Cheng and A. E. Meyerovich, *ibid.* **73**, 085404 (2006).
- <sup>16</sup>A. A. Abrikosov, *Fundamentals of the Theory of Metals* (North-Holland, Amsterdam, 1988).
- <sup>17</sup>G. Grimvall, *The Electron/Phonon Interaction in Metals* (Elsevier, Amsterdam, 1981).
- <sup>18</sup>G. Kästle, H.-G. Boyen, A. Schröder, A. Plettl, and P. Ziemann, *Phys. Rev. B* **70**, 165414 (2004).
- <sup>19</sup>V. B. Sandomirskii, *Sov. Phys. JETP* **25**, 101 (1967) [*Zh. Eksp. Teor. Fiz.* **52**, 158 (1968)].
- <sup>20</sup>G. Fischer and H. Hoffmann, *Solid State Commun.* **35**, 793 (1980); G. Fischer, H. Hoffmann, and J. Vancea, *Phys. Rev. B* **22**, 6065 (1980); L. A. Kuzik, Yu. E. Petrov, F. A. Pudonin, and V. A. Yakovlev, *Sov. Phys. JETP* **78**, 114 (1994) [*Zh. Eksp. Teor. Fiz.* **105**, 215 (1994)].
- <sup>21</sup>A. E. Meyerovich, *J. Low Temp. Phys.* **124**, 461 (2001).
- <sup>22</sup>R. M. Bowley and K. A. Benedict, *J. Low Temp. Phys.* **142**, 701 (2006).
- <sup>23</sup>B. Feldman, R. Deng, and S. Dunham, *J. Appl. Phys.* **103**, 113715 (2008).
- <sup>24</sup>A. E. Meierovich and B. E. Meierovich, *Sov. Phys. JETP* **66**, 833 (1987) [*Zh. Eksp. Teor. Fiz.* **93**, 1461 (1987)]; A. E. Meyerovich and D. Chen, *Phys. Rev. B* **66**, 235306 (2002); Y. Ke, F. Zahid, V. Timoshevskii, K. Xia, D. Gall, and H. Guo, *ibid.* **79**, 155406 (2009).
- <sup>25</sup>J. Rammer and H. Smith, *Rev. Mod. Phys.* **58**, 323 (1986).
- <sup>26</sup>R. C. Munoz, C. Arenas, G. Kremer, and L. Moraga, *J. Phys.: Condens. Matter* **15**, L177 (2003).
- <sup>27</sup>H. Marom and M. Eizenberg, *J. Appl. Phys.* **99**, 123705 (2006).
- <sup>28</sup>J. M. Purswani and D. Gall, *Thin Solid Films* **516**, 465 (2007).